Oxidase Reaction of Cytochrome cd_1 from *Paracoccus pantotrophus*†

Alrik Koppenhöfer,‡,§ Richard H. Little,‡,|| David J. Lowe,⊥ Stuart J. Ferguson,*,§ and Nicholas J. Watmough*,||

Department of Biochemistry, University of Oxford, South Parks Road, Oxford OX1 3QU, United Kingdom, Centre for Metalloprotein Spectroscopy and Biology, School of Biological Sciences, University of East Anglia, Norfolk NR4 7TJ, United Kingdom, and Biological Chemistry Department, John Innes Centre, Colney Lane, Norwich NR4 7UH, United Kingdom

Received August 16, 1999; Revised Manuscript Received December 2, 1999

ABSTRACT: Cytochrome cd_1 (cd_1NIR) from *Paracoccus pantotrophus*, which is both a nitrite reductase and an oxidase, was reduced by ascorbate plus hexaammineruthenium(III) chloride on a relatively slow time scale (hours required for complete reduction). Visible absorption spectroscopy showed that mixing of ascorbate-reduced enzyme with oxygen at pH = 6.0 resulted in the rapid oxidation of both types of heme center in the enzyme with a linear dependence on oxygen concentration. Subsequent changes on a longer time scale reflected the formation and decay of partially reduced oxygen species bound to the d_1 heme iron. Parallel freeze−quench experiments allowed the X-band electron paramagnetic resonance (EPR) spectrum of the enzyme to be recorded at various times after mixing with oxygen. On the same millisecond time scale that simultaneous oxidation of both heme centers was seen in the optical experiments, two new EPR signals were observed. Both of these are assigned to oxidized heme *c* and resemble signals from the cytochrome *c* domain of a "semi-apo" form of the enzyme for which histidine/methionine coordination was demonstrated spectroscopically. These observations suggests that structural changes take around the heme *c* center that lead to either histidine/methionine axial ligation or a different stereochemistry of bis-histidine axial ligation than that found in the as prepared enzyme. At this stage in the reaction no EPR signal could be ascribed to Fe(III) d_1 heme. Rather, a radical species, which is tentatively assigned to an amino acid radical proximal to the d_1 heme iron in the Fe(IV)-oxo state, was seen. The kinetics of decay of this radical species match the generation of a new form of the Fe(III) d_1 heme, probably representing an OH^--bound species. This sequence of events is interpreted in terms of a concerted two-electron reduction of oxygen to bound peroxide, which is immediately cleaved to yield water and an Fe(IV)-oxo species plus the radical. Two electrons from ascorbate are subsequently transferred to the d_1 heme active site via heme *c* to reduce both the radical and the Fe(IV)-oxo species to Fe(III)-OH^- for completion of a catalytic cycle.

Cytochrome cd_1 is a respiratory nitrite reductase enzyme for which the reaction product is nitric oxide. The enzyme is a dimer, with each monomer comprising two distinct domains, one of which contains a *c*-type cytochrome, the other a d_1 heme. The d_1 heme is a ferric dioxoisobacteriochlorin (*2*, *3*), a prosthetic group found exclusively in this class of bacterial enzyme. Structural studies confirm that the d_1 heme is the site of nitrite reduction (*4*), while the function of the *c*-type cytochrome is to mediate electron transfer from electron donor proteins to the active site. The crystal structures of the enzymes from both *Paracoccus pantotrophus*[1] and *Pseudomonas aeruginosa* have recently been solved to <2.15 Å (*5*, *6*). Both structures reveal the distance between the edges of the *c* and d_1 hemes within a monomer to be on the order of 12 Å with an angle between the hemes of approximately 60°, an arrangement that would appear to be consistent with fast electron transfer.

Paradoxically, an often commented upon feature of *P. aeruginosa* cd_1NIR[2] is the slow rate of electron transfer between hemes *c* and d_1 that is reported to be only on the order of a few per second. This result has been obtained either with no exogenous ligand bound to the d_1 heme iron (*7*) or with nitric oxide bound (*8*). Interestingly, cytochromes cd_1 can also catalyze the four-electron reduction of dioxygen to water (*9*). Some pre-steady-state kinetic studies of the oxidase reaction of the *P. aeruginosa* enzyme have been reported (*10*, *11*). An often overlooked result from this work is that with oxygen as a substrate the rate of electron transfer

† Supported by grants from the U.K. BBSRC (BO-5860), the Commission of the European Communities (BIO4-CT96-0281), and the Wellcome Trust (042103/Z/94/Z).

* To whom correspondence should be addressed. S.J.F.: Telephone +44 (1865) 275240; facsimile +44 (1865) 275259; E-mail ferguson@bioch.ox.ac.uk. N.J.W.: Telephone +44 (1603) 592179; facsimile +44 (1603) 592250; E-mail n.watmough@uea.ac.uk.

‡ These authors contributed equally to this work.

§ University of Oxford.

|| University of East Anglia.

⊥ John Innes Centre.

[1] Taxonomy of *Paracoccus pantotrophus*: This Gram-negative bacterium has at various times been considered either to be a monotypic species *Thiosphaera pantotropha* or a strain (GB17) of *Paracoccus denitrificans*. However, recent 16S RNA studies suggest that it should be regarded as a distinct species in the genus *Paracoccus*. Accordingly, it has been renamed *Paracoccus pantotrophus* (*1*).

[2] Abbreviations: cd_1NIR, cytochrome cd_1 nitrite reductase; EPR, electron paramagnetic resonance; HARC, hexaammineruthenium(III) chloride; k_{obs}, observed rate constant.

10.1021/bi991912k CCC: $19.00
Published on Web 03/11/2000

from the *c* to d_1 heme is much faster, taking place on the order of milliseconds. These kinetic studies of the oxidase reaction of the *P. aeruginosa* cd_1NIR have left many unanswered questions, including to what extent these findings can be extrapolated to the enzyme from *P. pantotrophus*. This is an important question, especially as it is now clear that the enzymes from the two sources have quite distinct structural features around the hemes (*5*, *6*).

The axial ligands of heme *c* in the oxidized *P. pantotrophus* enzyme as isolated are two histidine residues (His-17 and His-69). The proximal ligand of the d_1 heme is another histidine residue (His-200), while the distal ligand is a tyrosine residue (Tyr-25) provided by the cytochrome *c* domain. In contrast, the heme *c* in oxidized *P. aeruginosa* cd_1NIR has histidine (His-51) and methionine (Met-88) as axial ligands. Although the proximal ligand of d_1 (His-182) is equivalent to the histidine residue at position 200 in the *P. pantotrophus* sequence, the sixth ligand is a hydroxide ion. This distal hydroxide ion is hydrogen-bonded to a tyrosine residue (Tyr-10) from the other monomer; thus Tyr-10 is not equivalent to the tyrosine (Tyr-25) that provides the distal ligand to the d_1 heme iron in the *P. pantotrophus* enzyme (*5*, *6*).

Recently it has been shown that reduction of *P. pantotrophus* cd_1NIR results in a switching of ligands at the cytochrome *c* center such that the one of the histidine ligands (His-17) is replaced by a methionine residue (Met-106) (*4*). The result is a cytochrome *c* domain whose structure resembles that of the oxidized form of the *P. aeruginosa* cd_1NIR. Reduction of the *P. pantotrophus* enzyme also results in dissociation of Tyr-25 and the formation of a five-coordinate iron site at the d_1 heme to which nitrite (or dioxygen) can bind (*4*). These observations have been taken as evidence for a mechanism of nitrite reduction in *P. pantotrophus* cd_1 in which rebinding of Tyr-25 followed by nitrite reduction facilitates nitric oxide release from d_1 at the end of each catalytic cycle (*4*).

The publication of the structures of cytochromes cd_1 from the two bacteria, and the changes in structure that occur upon reduction of the *P. pantotrophus* enzyme, have raised many questions about the factors that influence the rate of heme−heme electron transfer in cd_1 nitrite reductases. Thus far the only study of heme−heme electron transfer in *P. pantotrophus* cd_1 used the technique of pulse radiolysis to reduce rapidly heme *c* and observe the subsequent internal electron-transfer events (*12*). This work showed heme−heme electron transfer to be relatively rapid ($k = 1.4 \times 10^3$ s^{-1}) and was interpreted in terms of an electron being transferred from bis-histidine-coordinated form of Fe(II) heme *c* to Fe(III) hexacoordinate d_1 (*12*).

Here we report a detailed study of the oxidase reaction of the *P. pantotrophus* cd_1NIR using a combination of stopped-flow visible absorption spectroscopy and freeze−quench EPR. The use of oxygen as electron acceptor avoids the complication of the potentially inhibitory product nitric oxide at the active site (*4*, *8*). The study was designed to determine the rates of electron transfer from the *c* to d_1 heme and seek evidence for intermediates of oxygen reduction.

MATERIALS AND METHODS

Purification of cd_1NIR from P. pantotrophus. Cytochrome cd_1NIR was purified essentially according to the method of Moir et al. (*13*) from the periplasm of a mutant strain of *P. pantotrophus* (M6) (*14*) grown under denitrifying conditions. A further column chromatography step (Sephacryl S-200 HR) was added to ensure homogeneous enzyme. The concentration of oxidized cd_1 was determined with the molar extinction coefficient of 2.85×10^5 M^{-1} at 406 nm for the dimer (*12*). The "semi-apo" form of *P. pantotrophus* cd_1 was prepared according to the method of Kobayashi et al. (*12*).

Spectroscopy. Electronic absorption spectra were recorded either on a Perkin-Elmer $\lambda 2$ spectrophotometer or on a Hitachi U-3000 spectrophotometer. EPR spectra were recorded on an X-band ER 200D spectrometer (Brucker Spectrospin) interfaced to an ESP 1600 computer and fitted with a liquid helium flow-cryostat (ESR-9, Oxford Instruments). In experiments to determine the *g*-value of the radical species, the microwave frequency was measured with a Marconi Instruments 20 GHz microwave counter model 2440.

Kinetic Measurements. The reaction of reduced cd_1 with oxygen was measured in an Applied Photophysics Bio-Sequential DX.17MV stopped-flow spectrophotometer with a 1 cm path length cell. Detection at a single wavelength was with a side window photomultiplier. In this configuration a minimum of 500 data points were collected per experiment. Detection at multiple wavelengths was with an Applied Photophysics photodiode array accessory. At least 200 spectra were collected per experiment with a maximum time resolution of 2.38 ms/spectrum.

Samples of reduced cd_1 were mixed with 600 μM dioxygen on a millisecond time scale in the freeze−quench apparatus previously described (*15*).

Oxygen-saturated buffer was obtained by passing a train of pure oxygen gas through a buffer solution at room temperature for a minimum of 30 min. Essentially oxygen-free solutions were obtained by the same method except that nitrogen gas was used rather than oxygen. The concentration of dissolved oxygen at 1 atm and room temperature was taken to be 1.2 mM (*16*). Subsaturating concentrations of oxygen were obtained by mixing oxygen-saturated and oxygen-free buffer solutions as required.

Treatment of Kinetic Data. The experimental traces recorded at single wavelengths were exported as ASCII files and analyzed as the sum of two or three exponentials with TableCurve 2D for Windows (Jandel Scientific, San Rafael, CA). Where appropriate, the time-resolved spectra were analyzed globally at all times and all wavelengths simultaneously. The analysis was performed on an Acorn A5000 personal computer using singular value decomposition (SVD) and global exponential fitting routines found in the software package Pro-K (Applied Photophysics, Leatherhead, U.K.).

RESULTS

Reduction of the Enzyme with Ascorbate plus HARC. A prerequisite for our kinetic studies of the reaction of reduced cd_1NIR with dioxygen was a reliable method of generating fully reduced enzyme. This can be prepared by treating oxidized cd_1NIR with excess dithionite. However, Parr et al. (*17*) observed that reduction of the *P. aeruginosa* enzyme in this fashion perturbed the spectrum of the Fe(II) d_1 heme, an observation that they attributed to bound sulfur oxyanions. This interpretation was borne out by a recent structural study

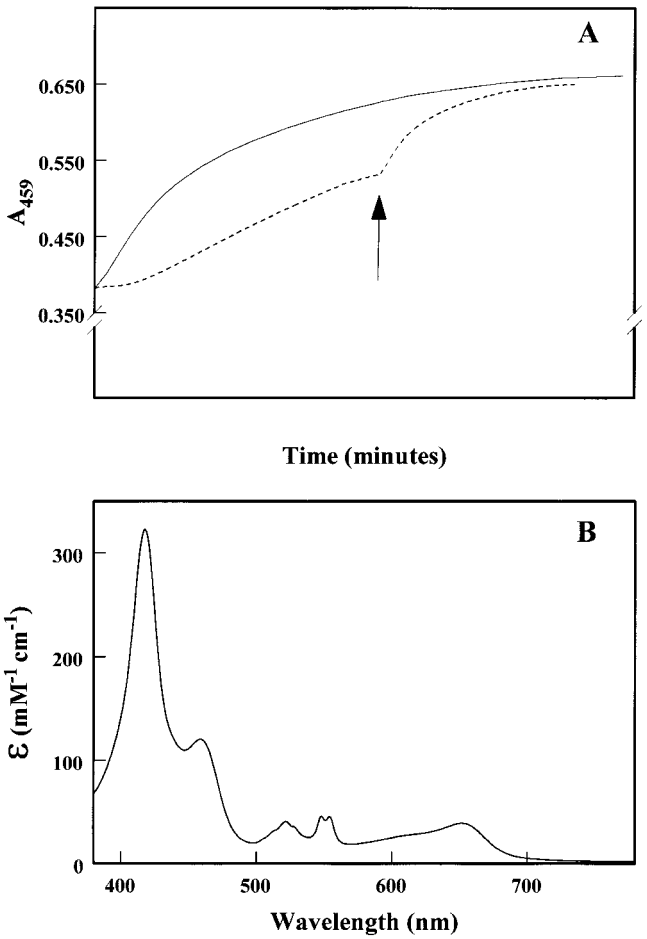

FIGURE 1: Reduction of *P. pantotrophus* cd_1NIR by ascorbic acid plus HARC. Samples of 6 μM cd_1NIR prepared in 50 mM potassium phosphate and 5 mM β-D-glucose, pH 7.0, were made anaerobic and any remaining traces of O_2 were removed by the addition of 500 milliunits of glucose oxidase/200 units of catalase. Panel A shows the time courses of reduction of cd_1NIR monitored at 459 nm initiated by the addition of (—) 2 mM ascorbate and 50 μM HARC or (- - -) 2 mM ascorbate followed by 50 μM HARC as indicated by the arrow. Panel B shows the electronic absorption spectrum of the sample used to obtain the record (—) in panel A 90 min after addition of 2 mM ascorbate and 50 μM HARC.

of dithionite-reduced *P. pantotrophus* cd_1NIR that showed sulfur dioxide bound at the d_1 heme iron (*4*). Such an initially bound ligand might compromise the subsequent reactions of fully reduced cd_1NIR (*18, 19*); therefore, we sought an alternative reductant.

It proved possible to reduce the enzyme with ascorbate plus HARC [hexaammineruthenium(III) chloride], although the rate of reduction was such that over 2 h was needed for reduction to be complete [Figure 1A (—)]. Omission of the HARC resulted in an even slower rate of reduction [Figure 1A (- - -)]. The rate of reduction by ascorbate plus HARC showed some pH dependence with the rate at pH 8.0 being 5-fold slower than at pH 6.0. The enzyme reduced in this way had an electronic absorbance spectrum (Figure 1B) characteristic of fully reduced cd_1NIR and was very similar to that obtained with methyl viologen (*4*).

Oxidation of Reduced cd_1NIR in the Presence of Oxygen. The visible absorption spectrum of cd_1NIR between 400 and 600 nm is complex because of overlap in the electronic transitions that arise from hemes *c* and d_1. Only at wavelengths greater than 600 nm can the absorbance be attributed solely to the d_1 heme. However, at 425 and 550 nm changes in absorbance essentially reflect the oxidation state of the heme *c*, while at 460 nm absorbance changes are dominated by the d_1 heme (*12*). Thus we chose these wavelengths, along with 640 nm, to monitor changes at both redox centers induced by the rapid mixing of reduced cd_1NIR with dioxygen in a stopped-flow spectrophotometer.

The rapid decrease in absorbance observed at both 425 and 550 nm in the first 500 ms following the mixing of reduced cytochrome cd_1 with a saturated solution of dioxygen (Figure 2, panels A and B) can be described by a single exponential (k_{obs} = ~30 s^{-1}). The amplitudes of the absorbance changes observed at these wavelengths indicate that oxidation of heme *c* is essentially complete. Following this burst of oxidation, we observed a much slower process during which a fraction (10%) of the heme *c* was rereduced. The reaction profiles over the first 500 ms observed at 460 and 640 nm were more complex (Figure 2, panels C and D). There was a rapid decrease in absorbance (k_{obs} = ~26 s^{-1}), which we attribute to oxidation of the d_1 heme, followed by a slower recovery of absorbance that reflects subsequent chemistry occurring at the d_1 heme.

This interpretation of the absorbance changes, seen at the four representative wavelengths shown in Figure 2, is consistent with the spectrokinetic analysis presented in Figure 3. The observed spectral changes that take place over the first 500 ms after mixing are illustrated in panel A of Figure 3. From these data we have used global analysis to calculate the spectra of the species that form (Y and Z) in the reaction of reduced cd_1NIR with oxygen (X):

$$X \rightarrow Y \rightarrow Z$$

The calculated spectrum of species **Y** [Figure 3B (•••)] clearly shows that heme *c* is now oxidized, an observation that would be consistent with heme−heme electron transfer on the millisecond time scale. The contribution of the d_1 heme to the spectrum of species **Y** is not the same as in the as-prepared oxidized enzyme, with diminished absorbance at 460 nm and a single band at around 640 nm in the visible region. The calculated spectrum of species **Z** [Figure 3B (- - -)] shows that heme *c* remains oxidized but that the heme d_1 spectrum has changed with increases in absorbance at both 460 and 650 nm, suggesting that further chemistry is taking place at this center.

Dependence of the Reaction upon [O_2]. The rate of the first rapid phase of oxidation (**X** → **Y**) was determined as a function of dioxygen concentration. A plot of k_{obs} as a function of [O_2] was linear with a significant nonzero intercept (not shown). For a simple reversible binding process under pseudo-first-order reaction conditions, the observed rate constant k_{obs} is a function of the association and dissociation rate constants together with the concentration of ligand:

$$k_{obs} = k_{+1}[O_2] + k_{-1} \quad (1)$$

These relationships yield estimates for the bimolecular association rate constant ($k_{+1} = 5.5 \times 10^4$ M^{-1} s^{-1}) and the dissociation rate constant (k_{-1} = 6.5 s^{-1}). However, the spectrokinetic data presented in Figure 2 clearly show both hemes to be oxidized synchronously. Therefore, it is clear that at least two separate processes, oxygen binding to the

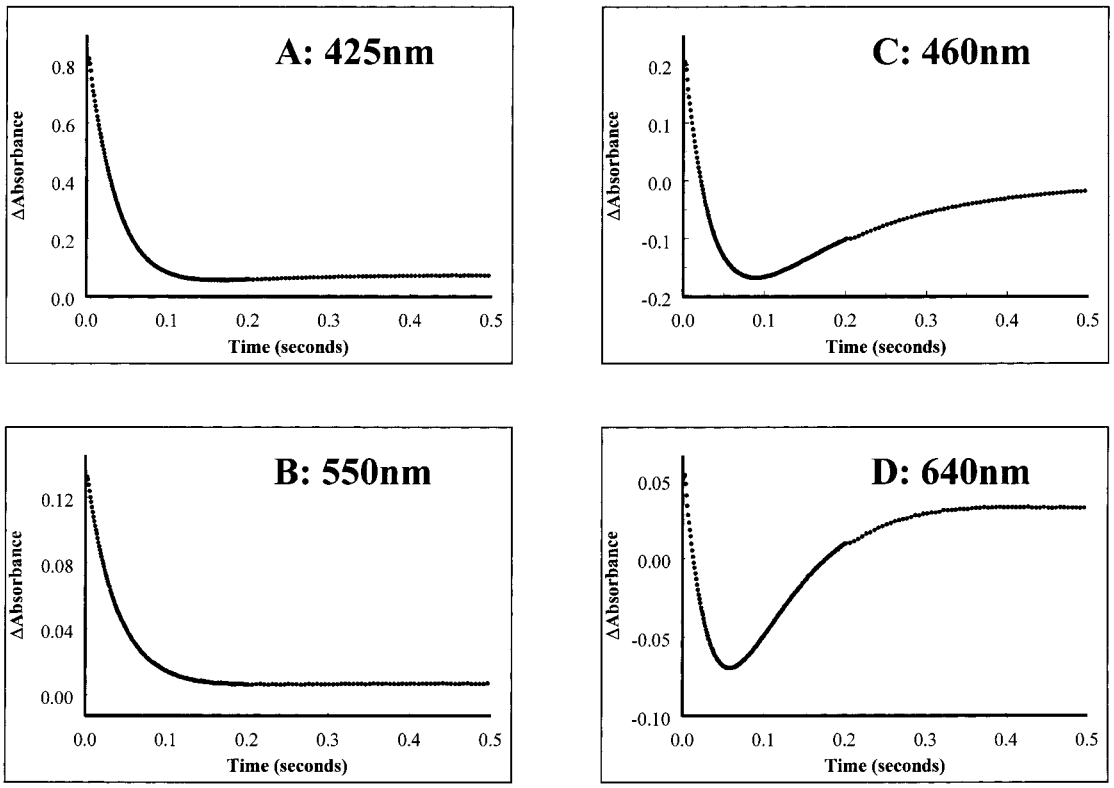

FIGURE 2: Reaction of cytochrome cd_1 with oxygen, monitored by stopped-flow spectrophotometry. cd_1NIR (6 μM) in 50 mM potassium phosphate, pH 6.0, was reduced by incubation with 5 mM ascorbate plus 50 μM HARC (20 °C) for 2 h. The reduced enzyme was mixed in the stopped-flow apparatus with an equal volume of the same buffer containing 1.2 mM O_2 (see Materials and Methods). The reactions were followed by using a split time base such that 200 data points were collected over the first 200 ms, followed by a further 200 data points over the following 0.8 s. The traces have been truncated after 0.5 s for clarity. The wavelengths chosen monitor the oxidation of the heme *c* center (425 nm, panel A, and 550 nm, panel B) or the d_1 heme center (460 nm, panel C, and 640 nm, panel D).

Fe(II) d_1 heme and heme−heme electron transfer, must take place on the time scale of what otherwise appears to be a single event.

To take account of the occurrence of two processes, a more rigorous treatment of the dependence of k_{obs} on $[O_2]$ is required. Equation 2 shows a general model (*20*) that can be used to describe the linked processes of substrate binding and heme-heme electron transfer:

$$\overset{\mathbf{X}}{c(\mathrm{II})d_1(\mathrm{II})} + O_2 \underset{k_{-1}}{\overset{k_{+1}[O_2]}{\rightleftharpoons}} \overset{\mathbf{X^*}}{c(\mathrm{II})d_1(\mathrm{II})-O_2} \xrightarrow{k_2} \overset{\mathbf{Y}}{c(\mathrm{III})d_1(\mathrm{III})-O_2^{2-}} \quad (2)$$

In this scheme the additional rate constant k_2 represents the rate constant for heme−heme electron transfer and K_{eq} is

$$K_{eq} = \frac{k_{+1}}{k_{-1}} \quad (3)$$

$$k_{obs} = \frac{k_2}{1 + (1/K_{eq}[O_2])} \quad (4)$$

The form of this equation is that of a rectangular hyperbole. However, if $k_2 > k_{-1}$ there will never be a significant accumulation of intermediate **X*** and the formation of Y will be rate-limited by the formation of the bimolecular complex (**X***). Under these circumstances the dependence upon $[O_2]$ of the measured rate constant (k_{obs}) for the overall reaction over the range 92−600 μM will appear to be linear. In contrast, for $k_2 < k_{-1}$ the dependence of k_{obs} upon substrate concentration would be described by a rectangular hyperbole even in this limited range of substrate concentrations. Simulated plots of k_{obs} versus $[O_2]$ (not shown) reveal that the minimum value of k_2 required to maintain an apparently linear relationship under the experimental conditions is of the order of 150 s^{-1} when the value of K_{eq} is constrained to 500 M^{-1}.

On longer time scales (>1 s) we observed a slow increase in absorbance at 550 nm that suggested that rereduction of heme *c* was taking place (Figure 3C). This was surprising given the sluggish reduction of the oxidized enzyme at pH 6.0, which took place over a period of approximately 2 h (Figure 1A). To investigate this further we recorded spectra at 0.65, 10.5, 30.2, and 60.3 s after mixing of reduced cd_1-NIR with dioxygen (Figure 3D). The spectrum recorded after 0.65 s [Figure 3D (—)] is very close to the calculated spectrum of species **Z** [Figure 3B (- - -)] and represents the product of the initial reaction of the reduced enzyme with dioxygen. However, in the spectra recorded at 10.5 s [Figure 3D (- - -)] and 30.2 s (Figure 3D (···)] there is an increase in absorbance at 550 nm, confirming that heme *c* becomes partially rereduced. In addition there are changes in the spectrum of the d_1 heme in the visible region with a decrease in absorbance at 650 nm and an increase in absorbance at 720 nm. The spectrum recorded at 60.3 s showed no further changes (data not shown).

Intermediates of Dioxygen Reduction. The question as to the chemical nature of the intermediates of oxygen reduction that are bound to the d_1 heme iron during turnover was

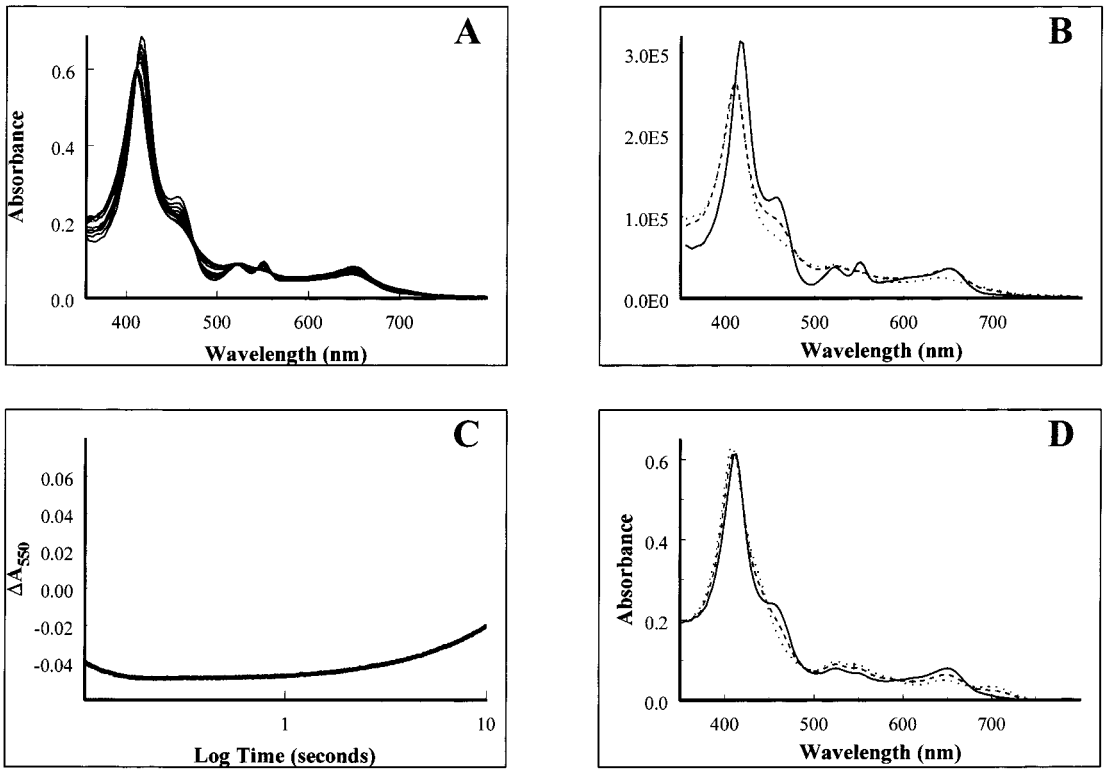

FIGURE 3: Spectrokinetic analysis of the reaction of reduced cd_1NIR with oxygen. The reaction was carried out as described in the legend to Figure 2 except that the stopped-flow spectrophotometer was fitted with a diode-array detector. Spectra recorded over the first 0.5 s are shown in panel A. The data were fitted by global analysis to the three-component model as described in the text, in which the spectrum of **X** was constrained to that of the fully reduced enzyme. The spectrum of **X** (—) together with the calculated spectra of the reaction intermediates **Y** (···) and **Z** (- - -) are shown in panel B. To observe the progress of the reaction on longer time scales, a second experiment was done in which 200 spectra were recorded over 60 s. Panel C shows the time courses of the absorbance changes at 550 nm (heme *c*) on a logarithmic time scale. Panel D shows spectra recorded at 0.65 s (—), 10.2 s (- - -), and 30.2 s (···).

addressed by use of freeze−quench EPR (Figure 4). On the same time scale as the simultaneous oxidation of both heme centers was seen in the optical experiments, we observed new signals arising from oxidized heme *c* (see later), but no signal that could be ascribed to ferric d_1 heme. However, we noticed the formation of an organic radical species (g = approx. 2.002, Figure 4) whose X-band EPR spectrum is shown in Figure 5. This radical species was readily apparent at 25 ms (Figure 4), reached its maximum intensity at 77 ms, and then decayed (Figure 4). There was no evidence of this radical species in the EPR spectra of fully reduced cd_1-NIR either before or after mixing with oxygen-free buffer (not shown).

The radical spectrum (Figure 5) is most intense at low temperature (8 K) and relatively high power (120 μW), which suggests that the radical lies close to a second paramagnet, presumably a metal and therefore probably one of the two hemes in cd_1NIR. The fine structure of the radical spectrum (Figure 5), which clearly shows splitting into five lines, is similar to that reported for a number of tyrosine radicals in metalloproteins (*21, 22*). All these features of the $g = 2.0033$ signal are inconsistent with the possibility of it arising from an ascorbate radical, which has a distinct two-line EPR spectrum, in the bulk phase.

After 77 ms the signal associated with the organic radical was fully developed (Figure 4), but neither heme was reduced (Figure 2) and there was no EPR signal that could be attributed to an isolated Fe(III) d_1 heme. This would suggest that the radical species is a feature of intermediate **Y**. The lack of an Fe(III) d_1 heme EPR spectrum, and the unusual relaxation properties of the organic radical, could be explained by intermediate Y containing d_1 heme in the Fe(IV)-oxo state. The disappearance of this radical species correlates well with the formation of a rhombic EPR spectrum ($g_x = 2.45$, $g_y = 2.22$, $g_z = 1.86$), which increased in intensity from 77 to 500 ms (Figure 4A). The closely spaced g-values of this rhombic species are very similar, but not identical, to the components of the spectrum arising from oxidized low-spin heme d_1 with histidine and tyrosine as axial ligands ($g_x = 2.52$, $g_y = 2.19$, $g_z = 1.84$) described by Cheesman et al. (*23*) (Figure 4B). These differences lead us to propose that the novel rhombic spectrum observed in the freeze−quench experiments arises from an Fe(III) low-spin d_1 heme with histidine and OH^- as axial ligands. There are two reasons for this assignment. First, such a compressed rhombic EPR spectrum is characteristic of an Fe(III) low-spin heme such as ferric dioxoisobacteriochlorin in which the ground-state electronic configuration is formally $(d_{xz}d_{yz})^4(d_{xy})^1$ (*23, 24*). Second, this species would be the expected product of the one-electron reduction of an Fe(IV)-oxo d_1 heme.

Nature of the Axial Ligands to Heme c. The freeze−quench EPR studies give insight into not only the events at the d_1 heme but also the nature of the axial ligands to heme *c*. The X-ray structure of the oxidized enzyme as prepared shows the *c*-type heme to have an unusual bis-histidine coordination, in which the planes of the imidazole groups are perpendicular to each other. This arrangement gives rise

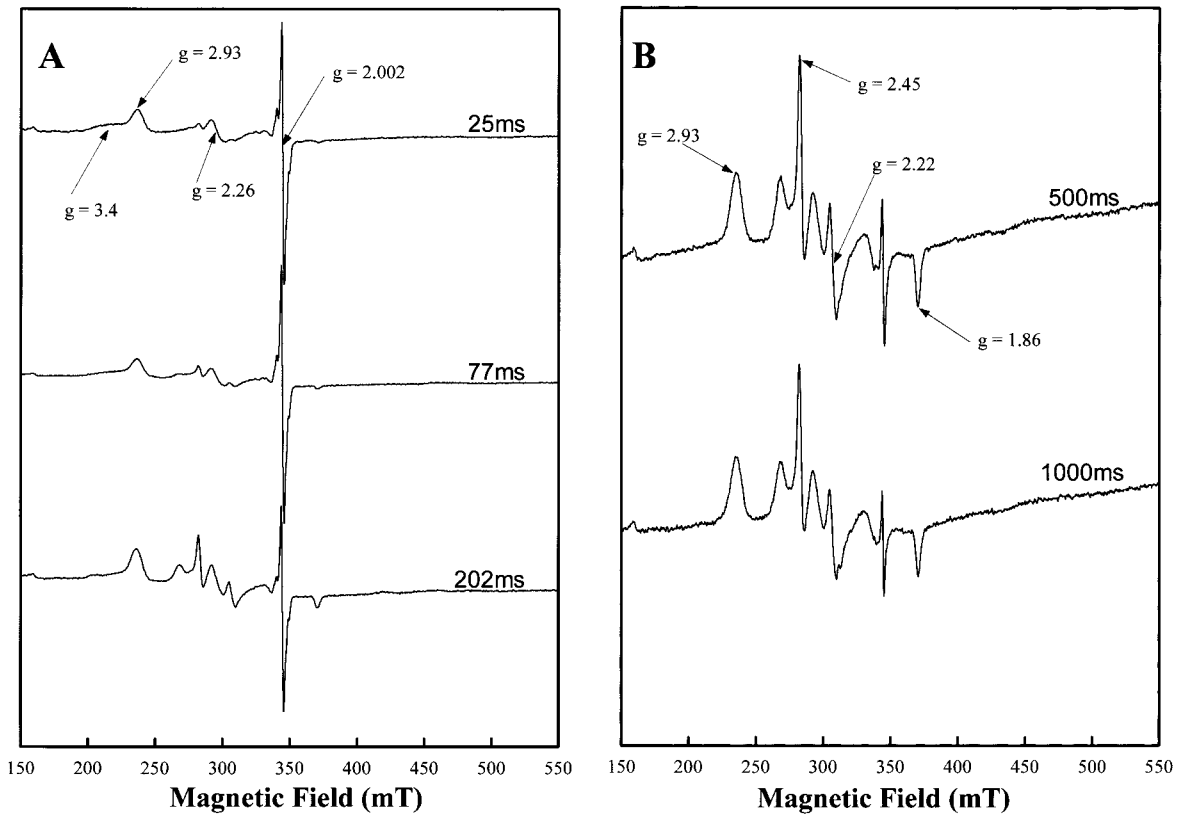

FIGURE 4: Progress of the reaction of reduced cd_1NIR with dioxygen, monitored by X-band EPR spectroscopy. Reaction conditions were essentially as described in the legend to Figure 2 except that the concentration of cd_1NIR was 60 μM and that, after mixing, samples were rapidly quenched by freezing at the time points shown according to the method of Bray et al. (*15*). Panel A shows spectra of samples frozen after 25, 77, and 202 ms. Panel B shows time points of 500 and 1000 ms (note the gain in panel B is 2.5 times that in panel A). Spectra were recorded at 10 K under the following conditions: microwave frequency 9.64 GHz, microwave power 2 mW, and modulation amplitude 1 mT.

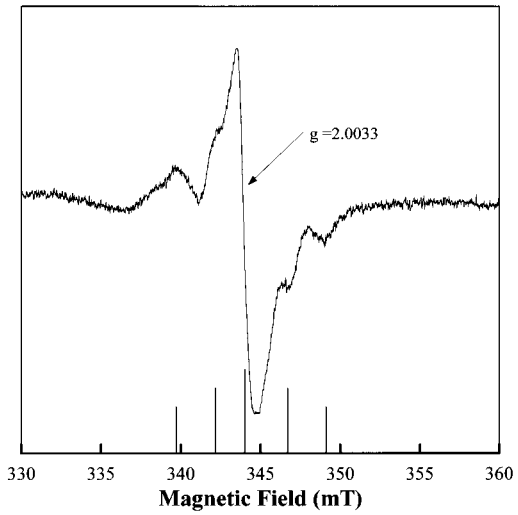

FIGURE 5: X-band EPR spectrum of the transient radical species seen during the reaction of reduced cd_1NIR with dioxygen. The EPR spectrum of the radical species trapped after 25 ms (Figure 4, panel A) was recorded at 5.5 K under the following conditions: microwave frequency 9.6404 GHz, microwave power 120 μW, and modulation amplitude 0.3 mT.

to a high g_{max}-type EPR signal of which only the g_z component can be seen at $g = 3.05$ (*23*) (Figure 6B). Within 25 ms of the reaction of the reduced enzyme with dioxygen, new EPR signals are seen. The major signals at $g = 2.93$ and $g = 2.26$ are presumed to be the g_z and g_y components of a rhombic trio that persists for at least 5 s (Figure 4 and data not shown). These values are close to those observed for the same components of the EPR spectrum arising from the heme *c* center of *P. aeruginosa* cd_1NIR (*23*), where the axial ligands are known from the crystal structure (*6*). A second minor EPR signal from the holoenzyme is also apparent in early time points (Figure 4A) as a broad shoulder centered at $g = 3.4$. This broad signal, which we have yet to assign, progressively disappears such that after 500 ms only the dominant $g = 2.93$ signal remains.

The EPR spectrum of the "semi-apo" form of the *P. pantotrophus* enzyme also contains two major features at $g = 2.92$ and $g = 2.26$. In this form of the enzyme, the d_1 heme has been chemically removed, leaving heme *c* as a single prosthetic group. "Semi-apo" cd_1NIR has an electronic absorption spectrum that contains a weak transition at 695 nm (Figure 6A), the position and intensity of which is characteristic of low-spin ferric hemes possessing at least one sulfur-containing ligand. Cytochrome *c* (histidine/methionine), bacterioferritin (bis-methionine) and cytochromes P-450 (cysteine/H_2O) all give rise to such intensity (*25*−*27*). The structures of the oxidized and reduced forms of the holoenzyme confirm that His-69 is adjacent to two cysteine residues (at positions 65 and 68) that covalently bind the vinyl groups of the heme. We assume that this ligand does not vary and that the sulfur ligand to the *c*-heme in the "semi-apo" enzyme is provided by Met-106 as in the reduced holoenzyme (*4*).

Our interpretation of the $g = 2.93$ and $g = 2.26$ signals that appear following oxygenation of the fully reduced

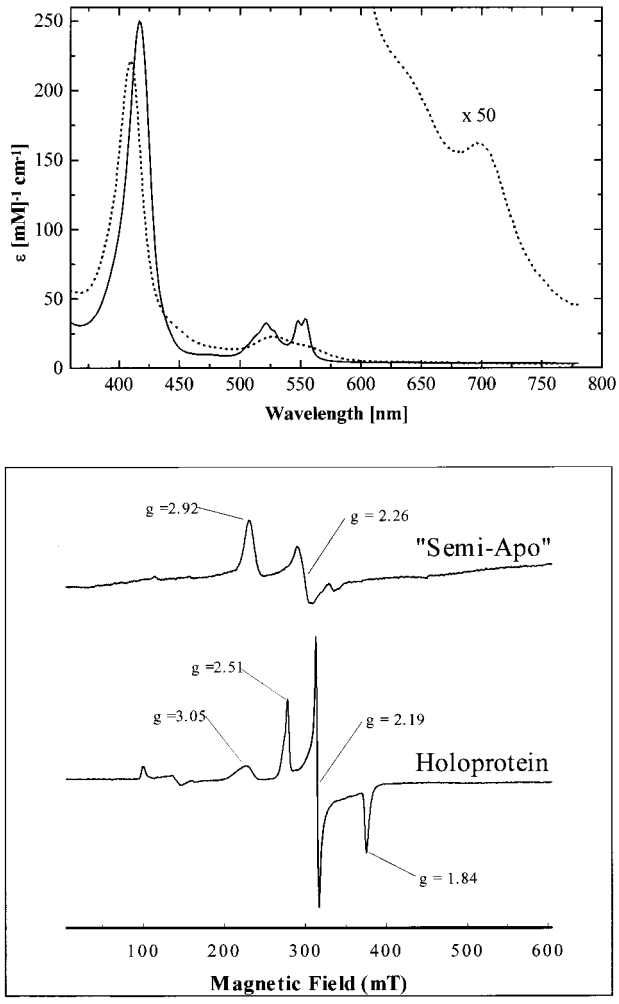

FIGURE 6: Electronic absorption and X-band EPR spectra of the "semi-apo" form of cd_1NIR. Panel A shows the room-temperature electronic absorption spectra of the oxidized (- - -) and dithionite-reduced states (—) of the "semi-apo" form of cd_1NIR. The protein concentration was 5 μM in 50 mM potassium phosphate buffer, pH 7.0. The absorbance between 600 and 800 nm is shown on a 50-fold expanded scale to illustrate the absorbance feature at 695 nm. Panel B shows the X-band EPR spectra of the fully oxidized states of the holo and "semi-apo" forms of cd_1NIR. The concentration of holo cd_1NIR was 700 μM and that of the "semi-apo" cd_1-NIR was 470 μm. Both samples were prepared in 50 mM potassium phosphate, pH 7.0. The spectra were recorded at 8 K under the following conditions: microwave frequency 9.44 GHz (holo cd_1-NIR) or 9.57 GHz ("semi-apo" cd_1NIR), microwave power 2.0 mW, and modulation amplitude 1 mT.

enzyme is that His-69 and Met-106 persist as axial ligands to heme *c*, at least on the time scale of our experiments, and that it is this form of heme *c* that gives rise to the new EPR signals. However, strictly speaking we cannot exclude that these two signals arise from a different arrangement of bis-histidine-coordinated heme *c* than that observed in the as-prepared enzyme. Work is currently in progress in our laboratories to try and discriminate between these two possibilities using magnetic circular dichroism (MCD) spectroscopy.

DISCUSSION

The reaction of cd_1NIR from *P. aeruginosa* with its various substrates has been studied by stopped-flow techniques over several years. The best-known result to emerge from this work is that the rate of electron transfer between the *c*- and d_1-type hemes is slow ($k_{obs} > 5\ s^{-1}$) compared to the likely rate of protonation of an oxygen atom on nitrite bound to the d_1 heme iron. The latter event generates water and a nitrosyl group bound to the ferrous state of the heme. The latter can be regarded as equivalent to an Fe(III)−NO complex from which the NO seems to dissociate slowly because a dead-end Fe(II)−NO complex forms even though the rate of electron transfer to the d_1 heme is slow (*8*). This slow rate of internal electron transfer from the *c* to the d_1 heme irons in cd_1NIRs is a matter of considerable interest, because in the absence of any structural changes, it is hard to reconcile with a distance of just 12 Å between the edges of the heme planes.

The cd_1NIR from *P. aeruginosa* also catalyzes an oxidase reaction, during which the rate of electron transfer from the *c* to d_1 heme is much faster, on the order of 100 s^{-1} (*11*). It has been uncertain to what extent this interesting, but often overlooked, result can be extrapolated to the *P. pantotrophus* cd_1NIR. This is especially true because it is now clear that the enzymes from the two sources have a number of quite distinct structural features. To address this issue we have used a combination of time-resolved spectroscopies to study the oxidase reaction of the *P. pantotrophus* cd_1NIR and show that, in common with the *P. aeruginosa* enzyme, interheme electron transfer occurs on the millisecond time scale when reduced *P. pantotrophus* cd_1NIR reacts with dioxygen.

The optical changes seen on mixing the fully reduced *P. pantotrophus* cd_1NIR with dioxygen are reminiscent of those reported by Greenwood et al. (*11*) for the same reaction in the *P. aeruginosa* enzyme. These authors monitored the reaction at 665 nm, although the absorbance maximum of *P. aeruginosa* cd_1NIR is in fact 650 nm, and observed a kinetic profile similar to that we report for the *P. pantotrophus* enzyme at 640 nm. In both enzymes the fast phase of the reaction, which is essentially complete in about 100 ms, involves bleaching of the absorbance associated with the reduced d_1 heme and the concomitant oxidation of the *c*-heme. Although Greenwood et al. noted that interheme electron transfer was rapid ($k > 100\ s^{-1}$), it is not a feature of their kinetic model (eq 1 of ref *11*). Consequently, the reported affinty of O_2 for the reduced d_1 heme ($K_a = 1 \times 10^4\ M^{-1}$), which is based upon an assumption of simple and reversible binding, may be an overestimate. Our preferred model for the *P. pantotrophus* enzyme involves the weak binding of oxygen to the Fe(II) d_1 heme and fast heme−heme electron transfer to reduce the bound oxygen to peroxide. A similar strategy is used by respiratory heme−copper oxidases to trap kinetically dioxygen (*28*).

Once the initial phase of oxidation is complete, we find no evidence of the type of low-spin Fe(III) d_1 heme with peroxide as the sixth axial ligand. Instead we see the formation of an organic radical that we have tentatively assigned to a tyrosine residue close to the d_1 heme iron. The distal ligand to the Fe(III) d_1 heme in oxidized cd_1NIR is Tyr-25 (*5*), but this is not necessarily the tyrosine that forms the radical since there is structural evidence that this residue moves away from the d_1 heme upon reduction (*4*). Instead we favor the participation of the conserved tyrosine at position 263, which is hydrogen-bonded to the d_1 heme macrocycle and only 6.5 Å away from the d_1 heme iron, which might account for the relaxation properties of the

radical that we observe.

Confirmation of the participation of a tyrosine radical in the oxygen cleavage chemistry would be significant. The rapid reduction of molecular oxygen to an Fe(IV)-oxo species plus water requires three electrons. Peroxidases (in which the substrate, peroxide, is already two-electron reduced) and oxidases use a variety of strategies to supply the third electron. These include oxidation of either the porphyrin macrocyle in horseradish peroxidase (HRP) (*29*) and ascorbate oxidase (*30*), a tryptophan residue in yeast cytochrome *c* peroxidase (CCP) (*31*), and a covalently modified tyrosine residue in cytochrome aa_3 (*32*). In each of these enzymes it is possible to generate the radical species in vitro for spectroscopic examination, but in each case turnover is sufficiently rapid to preclude direct observation of the participation of the radical in catalysis. The sluggishness of the cd_1NIR oxidase reaction allows observation of not only the formation and rereduction of the radical but also, in parallel spectrokinetic experiments, the formation and decay of an Fe(IV)-oxo species at the d_1 heme.

The rereduction of cd_1NIR that occurs subsequent to its initial oxidation (Figure 2) is important for understanding subsequent events that take place at the d_1 heme on longer time scales (Figures 3 and 4). If the reduction of cd_1NIR by ascorbate/HARC were always slow, as it is initially for the oxidized (as-prepared) enzyme, then rereduction of the enzyme would not be expected over the time course shown in Figure 4, in which case only two electrons would be available on each polypeptide chain. Since the structure shows that transfer of electrons between redox centers on different polypeptides in a dimer is unlikely because of distance considerations, then under these circumstances dioxygen bound to either monomer could not be fully reduced to two molecules of water. However, because we observe the formation and subsequent decay of the radical species, additional electrons must have been supplied to the d_1 heme center on the time scale of our experiments. If reduction of dioxygen is complete (i.e., four electrons are supplied to each polypeptide chain) then the final product formed could either be two waters or one water plus one bound hydroxide. This would be entirely consistent with our interpretation of the freeze−quench EPR spectra recorded at time points longer than 0.2 s. We have observed that reduction of the "semi-apo" enzyme, which has histidine/methionine coordination of the oxidized *c*-type center, by ascorbate is much faster than that of the holoenzyme. This would be consistent with the form of the holoenzyme generated immediately after oxidation of its *c*-type center being able to react faster with ascorbate, and thus gain additional electrons for the reduction of the initial species formed by the reaction of reduced cd_1NIR with oxygen, than the initial as-prepared state of the enzyme, which has bis-histidine coordination.

The time-resolved EPR spectra reported here (Figure 4) show the existence of an oxidized heme *c* center in *P. pantotrophus* cd_1NIR, the axial ligands of which are different from those observed in either the crystal or solution structures of the oxidized enzyme as prepared (*5*, *23*). The signals at $g = 2.93$ and $g = 2.26$ (Figure 4) are similar to signals reported in both the *P. aeruginosa* holoenzyme (*33*) and the *P. pantotrophus* "semi-apo" enzyme (Figure 6), both of which have histidine/methionine axial coordination. This strongly suggests that we have observed the same axial coordination for heme *c* in the reoxidized *P. pantotrophus* holoenzyme. It is important to realize that this observation implies that at least during turnover with oxygen, bis-histidine coordination of heme *c* depends on Tyr-25 being bound to the d_1 heme iron. When this cannot occur, as in the "semi-apo" enzyme, the heme *c* switches to histidine/methionine axial coordination, even in the oxidized state. The intermediate species Y and Z analyzed in this paper are each proposed to have an intermediate derived from O_2 bound to the d_1 heme iron. Thus one can expect this to result in the displacement of Tyr-25 in species Y and Z, an observation that would correlate with our proposal of histidine/methionine axial coordination for heme *c* in these species.

ACKNOWLEDGMENT

We thank the following: Professor M. T. Wilson, University of Essex, for his suggestions concerning the reaction mechanism, Professor A. J. Thomson and Dr. M. R. Cheesman, School of Chemical Sciences, UEA, for helpful discussions concerning the assignment of the EPR spectra, and Dr. D. J. Richardson, School of Biological Sciences, UEA, for his critical reading of the manuscript.

REFERENCES

1. Rainey, F. A., Kelly, D. P., Stackebrandt, E., Burghardt, J., Hiraishi, A., Katayama, Y., and Wood, A. P. (1999) *Int. J. Sys. Bacteriol. 49*, 645−651.
2. Chang, C. K. (1985) *J. Biol. Chem. 260*, 9520−9522.
3. Chang, C. K., and Wu, W. (1985) *J. Biol. Chem. 261*, 8593−8596.
4. Williams, P. A., Fülöp, V., Garman, E. F., Saunders, N. F. W., Ferguson, S. J., and Hajdu, J. (1997) *Nature 389*, 406−412.
5. Fülöp, V., Moir, J., Ferguson, S., and Hajdu, J. (1995) *Cell 81*, 369−77.
6. Nurizzo, D., Silvestrini, M. C., Mathieu, M., Cutruzzola, F., Bourgeois, D., Fülöp, V., Hajdu, J., Brunori, M., Tegoni, M., and Cambillau, C. (1997) *Structure 5*, 1157 1171.
7. Parr, S. R., Barber, D., Greenwood, C., and Brunori, M. (1977) *Biochem. J. 167*, 447−455.
8. Silvestrini, M. C., Tordi, M. G., Musci, G., and Brunori, M. (1990) *J. Biol. Chem. 265*, 11783−11787.
9. Timkovich, R., and Robinson, M. K. (1979) *Biochem. Biophys. Res. Commun. 88*, 649−55.
10. Wharton, D. C., and Gibson, Q. H. (1976) *Biochim. Biophys. Acta 430*, 445−453.
11. Greenwood, C., Barber, D., Parr, S. R., Antonini, E., Brunori, M., and Colosimo, A. (1978) *Biochem. J. 173*, 11−17.
12. Kobayashi, K., Koppenhöfer, A., Ferguson, S. J., and Tagawa, S. (1997) *Biochemistry 36*, 13611−13616.
13. Moir, J. W. B., Baratta, D., Richardson, D. J., and Ferguson, S. J. (1993) *Eur. J. Biochem. 212*, 377−85.
14. Berks, B. C., Richardson, D. J., Robinson, C., Reilly, A., Aplin, R. T., and Ferguson, S. J. (1994) *Eur. J. Biochem. 220*, 117−124.
15. Bray, R. C., Lowe, D. J., Capeillère-Blandin, C., and Fielden, E. M. (1973) *Biochem. Soc. Trans. 1*, 1067−1072.
16. Kaye, G. W. C., and Laby, T. H. (1966) p 153, Tables of Physical and Chemical Constants. Longmans, London.
17. Parr, S. R., Wilson, M. T., and Greenwood, C. (1974) *Biochem. J. 139*, 273−276.
18. Parr, S. R., Wilson, M. T., and Greenwood, C. (1975) *Biochem. J. 151*, 51−59.
19. Barber, D., Parr, S. R., and Greenwood, C. (1976) *Biochem. J. 157*, 431−438.

20. Bagshaw, C. R., Eccleston, J. F., Eckstein, F., Goody, R. S., Gutfreund, H., and Trentham, D. R. (1974) *Biochem. J. 141*, 351−64.
21. Ivancich, A., Jouve, H. M., Sartor, B., and Gaillard, J. (1997) *Biochemistry 36*, 9356−64.
22. Rigby, S. E., Nugent, J. H., and O'Malley, P. J. (1994) *Biochemistry 33*, 1734−42.
23. Cheesman, M. R., Ferguson, S. J., Moir, J. W. B., Richardson, D. J., Zumft, W. G., and Thomson, A. J. (1997) *Biochemistry 36*, 16267−16276.
24. Cheesman, M. R., and Walker, F. A. (1996) *J. Am. Chem. Soc. 118*, 7373−7380.
25. Cheesman, M. R., Kadir, F. H. A., Albasseet, J., Almassad, F., Farrar, J., Greenwood, C., Thomson, A. J., and Moore, G. R. (1992) *Biochem. J. 286*, 361−367.
26. Eaton, W. A., and Hochstrasser, R. M. (1967) *J. Chem. Phys. 46*, 2533−2539.
27. McKnight, J., Cheesman, M. R., Thomson, A. J., Miles, J. S., and Munro, A. W. (1993) *Eur. J. Biochem. 213*, 683−687.
28. Verkhovsky, M. I., Morgan, J. E., Puustinen, A., and Wikström, M. (1996) *Nature 380*, 268−270.
29. Dolphin, D., Forman, A., Borg, D. C., Fajer, J., and Felton, R. H. (1971) *Proc. Natl. Acad. Sci. U.S.A. 68*, 614−8.
30. Bonagura, C. A., Sundaramoorthy, M., Pappa, H. S., Patterson, W. R., and Poulos, T. L. (1996) *Biochemistry 35*, 6107−15.
31. Sivaraja, M., Goodin, D. B., Smith, M., and Hoffman, B. M. (1989) *Science 245*, 738−40.
32. MacMillan, F., Kannt, A., Behr, J., Prisner, T., and Michel, H. (1999) *Biochemistry 38*, 9179−9184.
33. Walsh, T. A., Johnson, M. K., Greenwood, C., Barber, D., Springall, J. P., and Thomson, A. J. (1979) *Biochem. J. 177*, 29−39.

BI991912K